Hyperspectral imaging for thermal effect monitoring in *in vivo* liver during laser ablation

M. De Landro, P. Saccomandi, *Member, IEEE*, M. Barberio, E. Schena, *Senior Member, IEEE*, M. J. Marescaux, M. Diana

***Abstract*— Thermal ablation is a minimally invasive technique used to induce a controlled necrosis of malignant cells by increasing the temperature in localized areas. This procedure needs an accurate and real-time monitoring of thermal effects to evaluate and control treatment outcome. In this work, a hyperspectral imaging (HSI) technique is proposed as a new and non-invasive method to monitor ablative therapy. HSI provides images of the target object in several spectral bands, hence the reflectance/absorbance spectrum for each pixel. This paper presents a preliminary and original HSI-based analysis of the thermal state in the *in vivo* porcine liver undergoing laser ablation. In order to compare the spectral response between treated and untreated areas of the organ, proper Regions of Interest (ROIs) were chosen on the hyperspectral images; for each ROI, the absorbance variation for the selected wavelengths (i.e., 630, 760, and 960nm, for deoxyhemoglobin, methemoglobin, and water respectively) was assessed. Results obtained during and after laser ablation show that the absorbance of the methemoglobin peaks increases up to 40% in the burned region with respect to the non-ablated one. Conversely, the relative change of deoxyhemoglobin and water peaks is less marked. Based on these results, absorbance threshold values were retrieved and used to visualize the ablation zone on the images. This preliminary analysis suggests that a combination of the absorbance information is essential to achieve a more accurate identification of the ablation region. The results encourage further studies on the correlation between thermal effects and the spectral response of biological tissues undergoing thermal ablation, for final clinical use.**

I. Introduction

Minimally invasive techniques have gained widespread recognition for tumor treatment as a potential alternative to conventional surgery. Among them, thermal ablations aim to produce the coagulative necrosis of the tumor by changing the tissue temperature using energy-based techniques (e.g., laser) [1]. The intraoperative monitoring of tissue temperature variations is crucial to ensure an effective therapy outcome [2]. Several thermometric techniques were proposed to guide ablation-based treatments in research, and more recently in clinical settings [3]. They can be divided into contact and contactless methods. Contact techniques require the use of physical sensors (e.g., fiber optic sensors, and thermocouples) directly inserted into the tissue [4]. Conversely, contactless methods exploit diagnostic imaging systems to provide the tissue temperature map without physical contact [2]. Magnetic Resonance is the only image-based technique recognized in clinical practice for thermal ablation monitoring. However, the high cost and the need for compatible tools limit its use. Other techniques have been investigated for research purposes, but they are not ready for clinical applications [5]. Hyperspectral imaging (HSI) could be a new tool to control tissue damage evolution during the ablation treatment. The spectral information provided with HSI allows the characterization of different types of biological tissues, whereas spatial information provides morphological data [6]. HSI has long been used in non-medical applications, including surveillance and target identification, agriculture, and space [7,8]. In the medical field, HSI has recently been applied to the investigation of physiologic and pathologic changes in animal and human tissues, to provide information regarding tissue state. The main emerging applications are peripheral vascular disease evaluation, diabetic foot ulcer prognosis, perfusion of gastrointestinal anastomoses, burn depth assessment, tumor detection, parathyroid discrimination during surgery [9–11]. Clancy et al. describe the use of this optical method to monitor porcine liver changes during microwave ablation. Multispectral imaging and diffuse reflectance spectroscopy were used to study the interplay between temperature rise and observed changes in tissue oxygen saturation *(StO_2)* [12]. The abovementioned investigation focuses only on StO_2 variation due to heat administration, even though other biological elements show a temperature dependence [13]. This paper aims to answer a similar medical need, proposing HSI as a potential method to monitor laser ablation outcome, and it expands the investigation of tissue components performances in response to temperature increase.

*This study was partly funded by the ARC Foundation for Cancer Research, via the ELIOS grant (P.I. Michele Diana). This project has received funding from the European Research Council (ERC) under the European Union's Horizon 2020 research and innovation program (GA n. 759159).

M. De Landro is with the Department of Mechanical Engineering, Politecnico di Milano, Milan, Italy (martina.delandro@polimi.it).

P. Saccomandi was with the Institute of Image-Guided Surgery, Strasbourg, France. She is now working at the Department of Mechanical Engineering, Politecnico di Milano, Milan, Italy (corresponding author e-mail: paola.saccomandi@polimi.it).

M. Barberio, M. Diana and J. Marescaux are with the Institute of Image-Guided Surgery, Strasbourg, France (manuel.barberio@ihu-strasbourg.eu).

E. Schena is with the Unit of Measurement and Biomedical Instrumentation, Università Campus Bio-Medico di Roma, Rome, Italy (e.schena@unicampus.it).

M. Diana and J. Marescaux are with the IRCAD, Research Institute against Cancer of the Digestive System, Strasbourg, France (michele.diana@ircad.fr, jacques.marescaux@ircad.fr).

978-1-5386-1311-5/19/$31.00 ©2019 IEEE

II. Theoretical Background

A. Hyperspectral imaging

In recent years, several researchers have targeted their efforts towards developing noninvasive optical diagnostic techniques by exploring the optical properties of tissues. Among the newer optical techniques, HSI is very promising for future medical applications. It consists in recording a series of biological tissue images in many adjacent narrow spectral bands and in reconstructing the reflectance spectrum for every pixel of the image [11]. The set of images subsequently obtained (typically tens or hundreds of images) is called *hypercube*. As a result, both spatial and spectral information about an object or scene under investigation can be obtained at the same time from the analysis of the hypercube [14]. The biggest advantage of this methodology is the contact-free spectroscopic measurement of an area without using contrast agents or other invasive procedures [15].

B. Peculiar wavelengths in tissue absorbance spectrum

The physical measurement principle of HSI consists in irradiating the tissue with white light and detecting the light remitted from the tissue [16]. Light entering biological tissue undergoes multiple scattering and absorption events as it propagates across the tissue [11]. Absorption and scattering characteristics change with tissue modification. Consequently, the light captured with HSI carries quantitative diagnostic information about the medium state [17]. Endogenous chromophores, such as hemoglobin, melanin, myoglobin, and water, are primarily responsible for the absorption of light in the wavelength region of 500-1000nm [18]. The measurement of the absorbance tissue spectrum can be used to identify and quantify the presence and relative concentrations of these tissue and skin chromophores [15]. For perfused tissues, the remission spectra are strongly dominated by the absorption of hemoglobin. Hemoglobin is the iron-containing protein in red blood cells. Under normal conditions, two types of hemoglobin are mainly present in the human blood circulatory system: oxyhemoglobin (HbO_2) and deoxyhemoglobin (Hb). The HbO_2 absorbance spectrum is characterized by a double peak structure in the range of 500 to 600nm, whereas the spectrum of Hb has only one peak in this spectral range. In the region between 600 and 1000nm, the spectra significantly differ, and the Hb shows a typical absorption band at 760nm. A third type of hemoglobin, methemoglobin ($metHb$), produced by a photo-induced oxidation of hemoglobin, is present in human blood under specific conditions. The reaction of $metHb$ formation is thermodynamically favorable and irreversible, but there is a barrier to the reaction requiring some minimum activation energy (heat) for initiation [19]. $MetHb$ is formed at temperatures above 65°C, with a maximum at approximately 72.5°C. It has characteristic absorption peaks at 404, 508, and 630nm [13]. In the 700 to 1000nm range, the absorption of water (H_2O) is dominant. It is characterized by peaks at 750, 830, and 960nm and increases significantly above 1000nm [15].

In this study, emphasis was put on quantifying changes in $metHb$, Hb and H_2O absorption peaks for the *in vivo* liver tissue during laser ablation. Measurements of diffuse reflectance were performed at different moments of the procedure and changes in optical response were evaluated. This evaluation aims at defining spectral features of specific tissue components, in order to select the best wavelengths for identifying the thermal damage induced by the laser.

III. Materials and Methods

A. Experimental set-up

The liver of one pig underwent a laser ablation procedure. In agreement with the ethical principle of Reduction, the animal was included at the end of a different experimental protocol at the Image-Guided Surgery Institute (IHU) of Strasbourg. The study received full approval from the Institutional Ethical Committee, in compliance with French laws for animal use and care and according to the European directives (2010/63/EU). After anesthesia, using 10cc of Propofol and 5cc of Esmeron (2% isoflurane was injected during the procedure), the pig (50kg) underwent a laparotomy, and the liver was exposed to perform the test.
The two optical fibers conveying the 1064nm laser light were inserted with needles (Figure 1.A), at 0.5cm below the liver surface. The laser ablation, performed at 2 W for 10 minutes, was recorded with a new hyperspectral camera system in a prototype status (TI-CAM, Diaspective Vision GmbH, Germany, Figure 1.B). Hypercubes were acquired with the Perception Studio software (Perception Park, Austria), which allows for a simultaneous acquisition in the 500 to 1000nm range, with a spectral resolution of 5nm. A CMOS camera unit at the spatial resolution of 640×480 pixels was used to record the scene. Data acquisition was performed in about 10 seconds. Six 120 W halogen lamps, equipped with diffusive reflectors, provide a uniform illumination of the entire investigation area [16]. The distance between the camera and the object was about 40cm. A desktop provided with the TIVITA suite image acquisition software is included in the apparatus as a user interface (Figure 1.C). To convert image data from radiance (spectral flux reaching the CMOS sensor) to reflectance (relation between the remitted light from an object and the light with 100% remission), the camera is calibrated with a white reference cube [15]. In order to have a reference measurement of thermal effects, superficial tissue temperature during laser ablation was collected using a thermal camera (FLIR, Figure 1.D).

B. Analysis of hyperspectral images

HSIs were acquired three times, namely before, during, and after the *in vivo* tissue laser ablation, in order to monitor

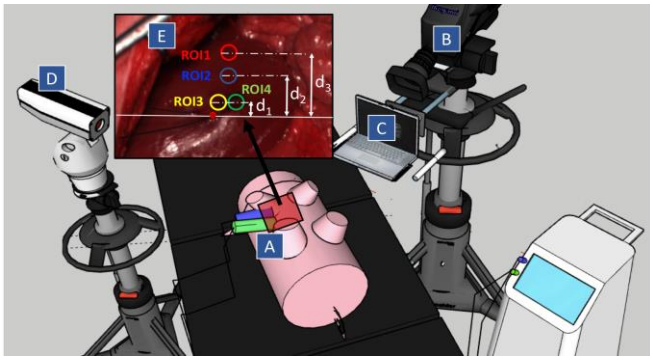

Figure 1: Experimental set-up for laser ablation in the pig, consisting in: A) two needles conveying the laser light, B) a hyperspectral camera, C) a laptop, D) a thermal camera. In E) a particle of the *in vivo* liver subjected to a laser ablation showing the location of ROIs is reported.

the absorbance change of the treated liver. Data analysis required the definition of four Regions of Interest (ROIs) for the hyperspectral images. Each ROI contains 172 pixels. As shown in Figure 1.E, ROI3, and ROI4 were placed in congruence with the ablation zone at d_1~30 pixels relative to the reported white axis, whereas ROI1 and ROI2 were in the region approximately at d_2~60 pixels and d_3~90 pixels respectively. Reflectance values measured for the pixels in the ROIs were averaged to obtain one characteristic reflection spectrum for each analyzed zone in the 500 to 1000nm range. Reflection data were converted in absorbance values with:

$$A = -log_{10}(R) \qquad (1)$$

where R is the averaged reflectance measured and A is the respective absorbance. Resulting absorbance spectra were examined in the following study.

IV. Results and Discussion

A. Absorbance spectra results

The obtained absorbance spectra are reported in Figure 2.

Peculiar wavelengths described in Section II.B are clearly visible in the tissue spectral response in all three acquisitions and regardless of the investigated zone. In the ablated region (ROI3-ROI4), peaks experience noticeable variation caused by the hyperthermal procedure.

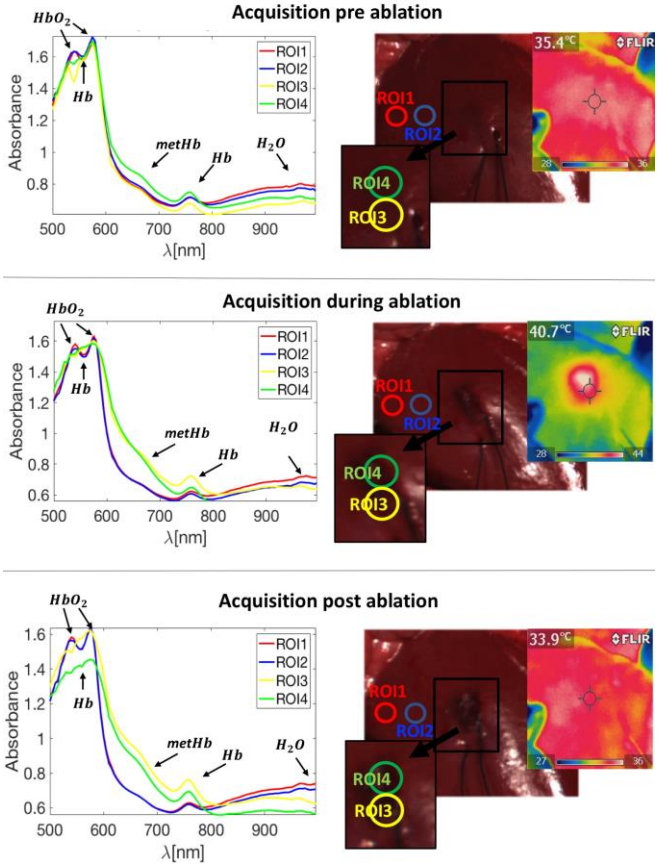

Figure 2: Absorbance spectra acquired prior to, during, and immediately after laser treatment in the 4 ROIs. Characteristic wavelengths, mentioned in Section II.B, for HbO_2, Hb, $metHb$ and H_2O are highlighted here. For each acquisition time, the RGB images showing the location of ROIs are reported together with thermal camera results exhibiting superficial tissue temperature values in the analyzed area.

Abnormal shapes for the hemoglobin peaks in a range out of the interest of the analysis (i.e., 500-600nm) are probably due to the ROI3 and ROI4 proximity to needles. This behavior was verified by evaluating spectra adjacent to the two laser applicators. In order to quantify $MetHb$, Hb and H_2O peaks of variation due to thermal ablation, absorbance responses for ROI2, ROI3 and ROI4 were evaluated relatively to ROI1 absorption values in the three measurement times (Figure 3). It can be noted that relative absorbance for the three wavelengths of interest changes once the ablation procedure starts. In addition, these variations do not disappear once the laser has been turned off. $MetHb$ peak shows the highest change, by reaching relative absorbance values in the 30 to 40% range for the treated zone. The following results confirm that an appropriate temperature increase will lead to $metHb$ formation [20]. Hb relative absorbance at 760nm also rises up to 20% in the ablated area, particularly in ROI3, less with respect to $metHb$. This is probably due to the conversion of HbO_2 into Hb with increasing temperature [21]. Relative absorbance peaks at 960nm exhibit negative values, in contrast to the response of the other analyzed chromophores. These relative variations are less marked and are probably due to H_2O evaporation.

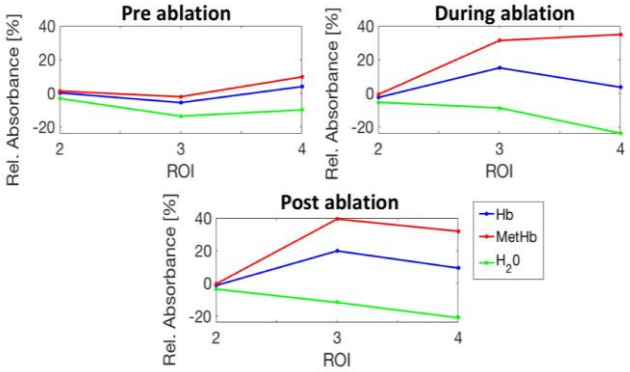

Figure *3*: Relative absorbance peak values in ROI2-ROI3-ROI4 for Hb at 760nm (blue), $metHb$ at 630nm (red), and H_2O at 960nm (green) obtained considering ROI1 as a reference for the non-ablated zone. Produced results are reported for the 3 acquisition times.

B. Tissue ablated detection

Starting from the analysis of the absorbance at the selected wavelengths, the appreciable distinction between spectral response in treated and untreated tissue was assessed. In this study, central wavelength for $metHb$, Hb and H_2O peaks were sorted to detect the ablated tissue. Absorbance peak values, 1.02 at 630nm, 0.73 at 760nm, and 0.58 at 960nm were used as thresholds in the three corresponding images acquired after the end of the procedure. Results, reported in Figure 4, show that images at each wavelength carry different information about the treated tissue. Additionally, the chosen thresholds (at 630 and 760nm) lead to the inclusion of needles in the detected area. In this respect, by considering the RGB image, it should be possible to identify and then exclude the non-target areas visible in it (such as artefacts, needle). A combination of the information at three different wavelengths could probably allow for a more comprehensive and accurate

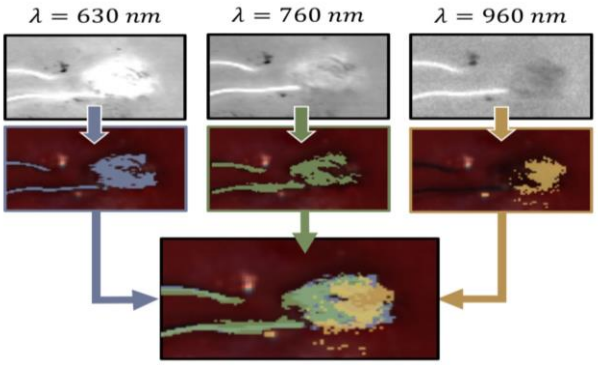

Fig. 4: On top, Hyperspectral images corresponding to the analyzed wavelengths showing the thermal effect of the laser ablation are shown. Detected pixels by using absorbance value at 630 nm (blue), at 760 nm (green) and at 960 nm (yellow) are provided. The combination of the three selected areas is reported. These results are overlapped to the RGB image acquired after the end of the procedure.

detection of the searched zone. For this purpose, a proper algorithm could be implemented to manipulate the acquired HSI data. By merging data provided with hyperspectral images, the loss of essential information and the error in the detection process should be reduced [22].

V. Conclusions

This study presents a preliminary analysis about the potential use of HSI output as a feedback to monitor thermal damage in tissues during thermal ablation. This investigation has highlighted that, during a laser treatment, the spectral response of the ablated tissue experiences a measurable variation, especially at specific wavelengths associated with tissue chromophores ($MetHb$, Hb and H_2O). Considering the central wavelength at which a change in the spectrum was noticeable, a prior attempt to visualize treatment-induced thermal damage was also made. An initial approach to analyze HSI data has been implemented, additional work would be useful to investigate more innovative and custom data processing techniques. Further experimental and theoretical analysis on the physiological phenomena underpinning the optical tissue behavior during ablation are also desired. Nevertheless, this first analysis has shown that the reflectance spectra obtained with the hyperspectral system provide additional information on the optical tissue behavior. Based on it, an innovative and harmless technique to optimize numerical models [22] or to help physicians in controlling the laser procedure could be implemented.

References

[1] M. Ahmed, C. L. Brace, F. T. Lee, and S. N. Goldberg, "Principles of and Advances in Percutaneous Ablation," *Radiology*, vol. 258, no. 2, pp. 351–369, 2011.

[2] P. Saccomandi, E. Schena, and S. Silvestri, "Techniques for temperature monitoring during laser-induced thermotherapy: an overview.," *Int. J. Hyperthermia*, vol. 29, no. 7, pp. 609–19, 2013.

[3] M. A. Lewis, R. M. Staruch, and R. Chopra, "Thermometry and ablation monitoring with ultrasound," *Int. J. Hyperth.*, vol. 31, no. 2, pp. 163–181, 2015.

[4] E. Schena, D. Tosi, P. Saccomandi, E. Lewis, and T. Kim, "Fiber optic sensors for temperature monitoring during thermal treatments: An overview," *Sensors (Switzerland)*, vol. 16, no. 7, pp. 1–20, 2016.

[5] E. Schena, P. Saccomandi, F. Giurazza, M. A. Caponero, L. Mortato, F. M. Di Matteo, F. Panzera, R. Del Vescovo, B. Beomonte Zobel, and S. Silvestri, "Experimental assessment of CT-based thermometry during laser ablation of porcine pancreas," *Phys. Med. Biol.*, vol. 58, no. 16, 2013.

[6] M. A. Calin, S. V. Parasca, R. Savastru, and D. Manea, "Characterization of burns using hyperspectral imaging technique - A preliminary study," *Burns*, vol. 41, no. 1, pp. 118–124, 2015.

[7] P. W. Yuen and M. Richardson, "An introduction to hyperspectral imaging and its application for security, surveillance and target acquisition," *Imaging Sci. J.*, vol. 58, no. 5, pp. 241–253, 2010.

[8] L. M. Dale, A. Thewis, C. Boudry, I. Rotar, P. Dardenne, V. Baeten, and J. A. F. Pierna, "Hyperspectral imaging applications in agriculture and agro-food product quality and safety control: A review," *Appl. Spectrosc. Rev.*, vol. 48, no. 2, pp. 142–159, 2013.

[9] B. Jansen-Winkeln, M. Maktabi, J. P. Takoh, S. M. Rabe, M. Barberio, H. Köhler, T. Neumuth, A. Melzer, C. Chalopin, and I. Gockel, "Hyperspectral imaging of gastrointestinal anastomoses," *Chirurg*, vol. 89, no. 9, pp. 717–725, 2018.

[10] M. Barberio, M. Maktabi, I. Gockel, N. Rayes, B. Jansen-Winkeln, H. Köhler, S. M. Rabe, L. Seidemann, J. P. Takoh, M. Diana, T. Neumuth, and C. Chalopin, "Hyperspectral based discrimination of thyroid and parathyroid during surgery," *Curr. Dir. Biomed. Eng.*, vol. 4, no. 1, pp. 399–402, 2018.

[11] G. Lu and B. Fei, "Medical hyperspectral imaging: a review," *J. Biomed. Opt.*, vol. 19, no. 1, p. 010901, 2014.

[12] N. T. Clancy, K. Gurusamy, G. Jones, B. Davidson, M. J. Clarkson, and J. David, "Spectral Imaging of Thermal Damage Induced During Microwave Ablation in the Liver," pp. 3001–3004, 2018.

[13] L. L. Randeberg, J. H. Bonesrønning, M. Dalaker, J. S. Nelson, and L. O. Svaasand, "Methemoglobin formation during laser induced photothermolysis of vascular skin lesions," *Lasers Surg. Med.*, vol. 34, no. 5, pp. 414–419, 2004.

[14] M. A. Calin, S. V. Parasca, D. Savastru, and D. Manea, "Hyperspectral imaging in the medical field: Present and future," *Appl. Spectrosc. Rev.*, vol. 49, no. 6, pp. 435–447, 2014.

[15] A. Holmer, J. Marotz, P. Wahl, M. Dau, and P. W. Kämmerer, "Hyperspectral imaging in perfusion and wound diagnostics - Methods and algorithms for the determination of tissue parameters," *Biomed. Tech.*, 2018.

[16] A. Holmer, F. Tetschke, J. Marotz, H. Malberg, W. Markgraf, C. Thiele, and A. Kulcke, "Oxygenation and perfusion monitoring with a hyperspectral camera system for chemical based tissue analysis of skin and organs," *Physiol. Meas.*, vol. 37, no. 11, pp. 2064–2078, 2016.

[17] M. C. Pierce, R. A. Schwarz, V. S. Bhattar, S. Mondrik, M. D. Williams, J. J. Lee, R. Richards-Kortum, and A. M. Gillenwater, "Accuracy of in vivo multimodal optical imaging for detection of oral neoplasia," *Cancer Prev. Res.*, vol. 5, no. 6, pp. 801–809, 2012.

[18] R. Richards-Kortum and E. Sevick-Muraca, "Quantitative Optical Spectroscopy for Tissue Diagnosis," *Annu. Rev. Phys. Chem.*, vol. 47, no. 1, pp. 555–606, 1996.

[19] J. Kehlet, G. Frangineas, H. Pummer, J. F. Black, and J. K. Barton, "Cooperative Phenomena in Two-pulse , Two-color Laser Photocoagulation of Cutaneous Blood Vessels Cooperative Phenomena in Two-pulse , Two-color Laser Photocoagulation of Cutaneous Blood Vessels," *Image (Rochester, N.Y.)*, vol. 73, no. 6, pp. 642–650, 2001.

[20] S. Kimel, B. Choi, L. O. Svaasand, J. Lotfi, J. A. Viator, and J. S. Nelson, "Influence of laser wavelength and pulse duration on gas bubble formation in blood filled glass capillaries," *Lasers Surg. Med.*, vol. 36, no. 4, pp. 281–288, 2005.

[21] H. Jia, B. Chen, and D. Li, "Dynamic optical absorption characteristics of blood after slow and fast heating," *Lasers Med. Sci.*, vol. 32, no. 3, pp. 513–525, 2017.

[22] D. A. Gil, L. M. Swift, H. Asfour, N. Muselimyan, M. A. Mercader, and N. A. Sarvazyan, "Autofluorescence hyperspectral imaging of radiofrequency ablation lesions in porcine cardiac tissue," *J. Biophotonics*, vol. 10, no. 8, pp. 1008–1017, 2017.